LJMU Research Online

Chen, Y, Chen, X, Xu, X and Yu, G

Quantitative impacts of regenerative vibration and abrasive wheel eccentricity on surface grinding dynamic performance

http://researchonline.ljmu.ac.uk/8198/

Article

http://researchonline.ljmu.ac.uk/

Quantitative Impacts of Regenerative Vibration and Abrasive Wheel Eccentricity on Surface Grinding Dynamic Performance

Yong Chen [1, 2, a]   Xun Chen [3, b]   Xipeng Xu [2, c]   Ge Yu [4, d]

[1]College of Mechanical Engineering and Automation, Huaqiao University, Xiamen, 361021, China

[2]Ministry of Education Engineering Research Centre for Brittle Materials Machining, Xiamen, 361021, China

[3]General Engineering Research Institute, Liverpool John Moores University, Liverpool L3 3AF, U.K.

[4]Roll forging institute, Jilin University, Changchun, 130025, China

[a]chenyong@hqu.edu.cn, [b]x.chen@ljmu.ac.uk, [c]xpxu@hqu.edu.cn, [d]yuge@jlu.edu.cn

Abstract

In grinding, regenerative-vibration and forced-vibration due to grinding wheel eccentric rotation are main excited-vibration sources that interact with grinding material removal mechanism. In the paper, instantaneous undeformed chip thickness in down-grinding cutting phase may consist of two components, i.e. linear kinetic thickness and nonlinear dynamic thickness. Considering abrasive grit-workpiece interaction in the grinding contact zone, the grinding vibration system is presented by a new set of differential equations of two degrees of freedom (DOF) with a close-loop feedback control system models. Conventional grinding control parameters, including wheel spindle speed, work-speed in feed direction and radial cutting depth, are often regarded as linear constants in many existing simplified models. When considering time delay, they can be transferred to nonlinear variables, so the capability of prediction and the accuracy of solution of the grit-workpiece dynamics performance are improved. Based on quantitative comparison of force and vibration magnitudes, the influence of the eccentric rotation of abrasive wheel and the negative rake angle of working grit cutting edges on grinding performance are demonstrated in the paper.

Keywords: surface grinding, vibration system, dynamics characteristics, regenerative vibration, wheel eccentricity

Nomenclature

a_e depth of cut(um)

c modal damping of machine-wheel-workpiece system ($N \cdot s/um$)

c_s grinding ratio of tangential force and radial force

dF_{xi}, dF_{yi} instantaneous forces on a single-grit in normal direction and in feed direction(N)

dF_{ti}, dF_{ri} instantaneous tangential and radial forces on a single-grit in shear plane(N)

R, d_s grinding wheel radius and grinding wheel diameter(mm)

f_t feed per revolution of single grit(um)

$G_{xx}(s)$ 、 $G_{xy}(s)$ 、 $G_{yx}(s)$ 、 $G_{yy}(s)$ direct and cross transfer functions of machine-wheel-workpiece vibration system in the normal and feed directions

$H_{cu,0}(s)$ kinetic undeformed chip thickness in frequency domain(um)

$H_{cu}(s)$ final grinding undeformed chip thickness in frequency domain (um)

$H_{is}(t), H_{is}(t-T)$ dynamic displacement of current and previous grits in radial direction(um)

$H_{iw}(t), H_{iw}(t-T)$ dynamic displacement of current and previous workpieces in radial direction(um)

k modal stiffness of machine-wheel-workpiece system (N/um)

K_s grinding force ratio in per unit chip area at micro-grinding condition

m modal mass of machine-wheel-workpiece system($N \cdot s^2/um$)

n active grit numbers in the interaction zone

$R_i'(\varphi_i'), R_{i-1}'(\varphi_i')$ grinding radius of the current and previous working grits in contact zone(um)

$h_{cu,0}$ kinetic undeformed chip thickness (um)

$h_{cu,i}(\varphi_i)$ instantaneous undeformed chip thickness of single grit(um)

P_m specific grinding energy of removing material per unit volume($J.mm^{-3}$)

T discrete time interval between current and adjacent working grits(s)

$\Delta h_{cu,i}$ dynamic undeformed chip thickness derived from regenerative vibration(um)

V_w feed speed of workpiece(mm/s)

V_s peripheral speed of grinding wheel (m/s)

x,y,z position coordinates(m)

$X_i(t), X_i(t-T), Y_i(t), Y_i(t-T)$ dynamic displacements of current and previous grit-workpiece pairs in normal direction and in feed direction with Cartesian coordinate(um)

δ_e wheel eccentricity value(um)

$\delta h_{cu,i}(\varphi_i)$ eccentric undeformed chip thickness deviation (um)

ε comprehensive influential coefficient of friction behaviour

φ_i rotational position angle of single grit($degree$)

φ_{ei0} initial position angle of grit i on abrasive wheel($degree$)

φ_e relative position angle with actual wheel rotational centre($degree$)

ω angular velocity of abrasive wheel ($degree/s$)

θ rotational angle of spindle of abrasive wheel($degree$)

Ω entire included angle of grit in interaction zone($degree$)

Ψ angle deviation between two subsequent finished surface undulations($degree$)

γ_0 negative rake angle of single grit($degree$)

ξ_{Fx}, ξ_{Fy} change ratio of grinding forces in normal direction and in feed directions

$\xi_{\Delta x}, \xi_{\Delta y}$ change ratio of grinding vibrations in normal direction and in feed directions

1. Introduction

As one of primary manufacturing methods, grinding is still a prime method to achieve stable high quality products. In contrast to other machining operations, such as milling, turning and drilling, the material removal mechanism in grinding and the interactions between grits and workpiece are much more complex to be characterized accurately due to a multitude of irregularly shaped, randomly positioned abrasive grits on the circumference of a grinding wheel [1, 2, 3]. Due to the complex distribution and characteristic of abrasive grits, the fundamental of grinding dynamics and its impact on ground surface have not yet been fully explored from a holistic and systemic perspective. Under the complicated grinding conditions, it is difficult to present a chip formation by a simple fixed geometric-kinematic interaction [4, 5]. Grinding vibration coupled with many nonlinear mechanisms, including self-excited and forced-vibration, is considered as a major factor to deteriorate grinding precision and shorten the wheel life, leading to poor surface roughness, excessive machine tools wear and associated breakdown [6]. As a result of grinding vibration, the unstable machining system generally leads to production losses and high rejection rates of products. To avoid or eliminate the influence of grinding vibration, especially chatter, many automatic control strategies with online compensation algorithms and offline optimization techniques are developed and evolved in the last decades [7,8].

Numerical models considering geometrical and kinetic factors in material removal have been developed to reveal the linear or nonlinear functional correlation between the process control parameters and the machining system characteristic variables by using the methods of finite element method (FEM), molecular dynamics(MD), empirical model fitting and dynamic grey system models [1, 4~6, 9,10]. Many of these methods are based on scratching or grinding tests with a single or a cluster of CBN, diamond grits. The chip formation mechanism is inferred from a large amount of experimental and simulation data analyses. Because of stochastic nature of wheel topography, the grit distribution and material characteristics under specific test conditions cannot be controlled and monitored easily, the dynamic grinding performance and its control mechanism are typically judged qualitatively [11,12,13].

The material removal process in a grinding process is conducted by a large number of cutting edges of grits. It has been generally accepted that the material removal during the engagement of an abrasive grit with the workpiece material has three phases, i.e. rubbing, ploughing and cutting [1, 4, 5, 6, 10, 11]. By increasing cutting depth of grits, the material removal is more effective due to the increased cutting actions in the engagement of grits and workpiece [5]. A typical material flow trajectory of surface grinding traditional metallic material, such as low-carbon steel or medium-carbon steel is illustrated in Figure 1 [14, 15]. Looking at grit shape, a larger negative rake angle of grit leads to greater plastic deformation of machined materials. A common method for the investigation of material deformation flow during grinding is a single grit scratching test in considering the negative rake angle of grit as depicted by the variable γ_0 which is equal to the half of apex angle of the grit. The deformed metallic material around rake face of grit is moving upwards, which is divided in two parts. One part of the material flows under the bottom of single grit. The other part of the material moves up in the opposite direction to form chip. There is a critical transition point that is depicted as "breaking point" shown in Figure 1 at the rake face, where the material flow separated. With the increasing absolute value of negative rake angle of grit cutter, the longer length between the transition point and the apex of single grit is observed with more severe plastic deformation. By further increasing the penetration depth of the grit, the material removal is enhanced due to the effective rake angle of grit cutter becomes more positive leading to more cutting actions. In addition, the orientation of the abrasive grit (e.g. grit shape orthogonal to

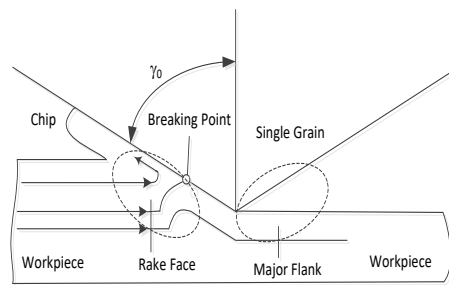the feed direction) has an influence on chip formation behaviour [2, 3, 9, 12].

Fig. 1 Material flow trajectory of single grit with negative rake angle γ_0

During forced-excited grinding, the dynamic influence of eccentrically rotated grinding wheel is significant in the abrasive grit-material contact zone and cannot be neglected in the analytical model of grinding force. Although there are a few form errors caused by big grits with complex distribution density, as well as non-uniform thickness of wheel with poor manufacturing quality, the geometrical errors of abrasive wheel could be eliminated regularly by dressing or truing procedure prior to grinding. However, dynamic eccentric errors acting on abrasive wheel during grinding that derive from many unavoidable factors, such as uncontrollable clamping deviation between the wheel and spindle assembly(e.g. common value of clamping accuracy in precision grinding is limited strictly in the range of 1 *um*), unbalanced rotational and vibrationary transmission effect resulted from machine tool spindle even with high stiffness, and unavoidable real-time wear eccentricity of abrasive wheel, cannot be eliminated thoroughly on-line during actual process.

The dynamic undeformed chip thickness and machining behaviours at grinding-in or grinding–out conditions would result in significant variation no matter the wheel eccentricity is implemented or not. Especially, the randomly and irregularly relative errors excited from intermittent impact between abrasive wheel and workpiece are main external influential factor on grinding instability. The complex influence mechanism on grinding dynamics is necessary to be studied deeply to improve applicability and accuracy of analytical models of grinding force and vibration. Badger et al analysed how grinding-wheel untruth or non-circular shape affects forces, wheel wear and temperatures and developed a model to predict final scallop-profile shape from grinding parameters and eccentricity[16]. Inasaki et al presented origin of chatter that is due to regenerative mechanism during cylindrical, surface and internal grinding process and discussed the effect of run-out on chatter as a function of material-removal rate along with an optical sensor to measure run-out[7]. Altintas et al reviewed non-linearities in the stability models and presented dynamic time domain model of transverse and plunge grinding[8]. Whenever these researches are conducted, the quantitative accuracy evaluation of the influential mechanism on the dynamic characteristics of surface grinding is critical for the indication of machining stability. This paper attempts to reveal that situation.

So far, geometries of abrasive grits are always assumed to be either pyramid cones with designated angles or simple sphere or ellipsoid [4,9,13]. While they are not same as aforementioned ideal standard geometries in actual grinding process, effective grits penetrating-in material can be measured with the development of test technology and be dimensioned accurately as geometries of pyramid or truncated tetrahedron with defined angle in different interaction interfaces between abrasive grits and workpiece, including depicted top opening angle, apex angle in feed direction, negative rake angle, wedge angle etc [17, 18, 19]. When assessing the influence of the grit shape characteristics on chip formation, negative rake angle of single grit has the greatest influence on the

chip formation or penetration depth, as well as undeformed chip thickness of the grit by comparing with the other influence factors[17,19].

Considering down-grinding process , a set of improved analytical models of grinding dynamics in views of chip formation mechanism are developed in this paper to illustrate the comprehensive influence of the eccentricity of grinding wheel and regenerative vibration as nonlinear characteristics. Moreover, the close-loop feedback system are proposed for the regenerative vibration process analysis. While the grinding process control parameters, such as wheel spindle rotational speed, grinding speed and chip thickness are normally regarded as linear constants, it will be more accurate and realistic to consider these parameters as nonlinear variables in the wheel-workpiece dynamics close-loop feedback control system. Therefore the quantitative comparison of force and vibration magnitudes are conducted in this paper under the influence of the eccentric rotation of abrasive wheel and the negative rake angle of working grit cutting edges on grinding performance. Furthermore, the influential mechanism identified could be used to predict ground surface topography formation and to assess the distribution characteristics of grinding chip thickness.

2. Analytical models of grinding dynamics characteristics

2.1 Improved mathematical models of instantaneous undeformed chip thickness

It has been recognised that grinding chip formation parameters directly affect the process behaviour and finished surface precision [1, 2, 5，6, 10, 15]. The grinding chip formation parameters can be calculated in terms of grinding kinematics relationship. There are two typical types of grinding process, i.e. up grinding and down grinding, as illustrated in Figure 2. Considering an ideal process and a spring-mass-damper contact system, abrasive grits continuously increase (up-grinding) or decrease (down-grinding) undeformed chip thickness in their engaging cycles with the workpiece. Here, ideal material removal process is assumed, which means rubbing and ploughing behaviour of material are not considered and each rigid grit with shape of pyramid removes the whole material volume encountered. With consideration of effects of regenerative vibration mechanism and circumferential eccentric errors of wheel profile that result in the changes of undeformed chip thickness and ground surface profile, the instantaneous chip thickness $h_{cu,i}(\varphi_i)$ at the cross-section of single grit along the Z-direction(wheel axial direction) are comprised of three factors: (a) the kinematic static undeformed chip thickness used in many previous research works, (b) dynamic chip thickness and (c) dynamic chip thickness deviation calculated as Equations 1 and 2.
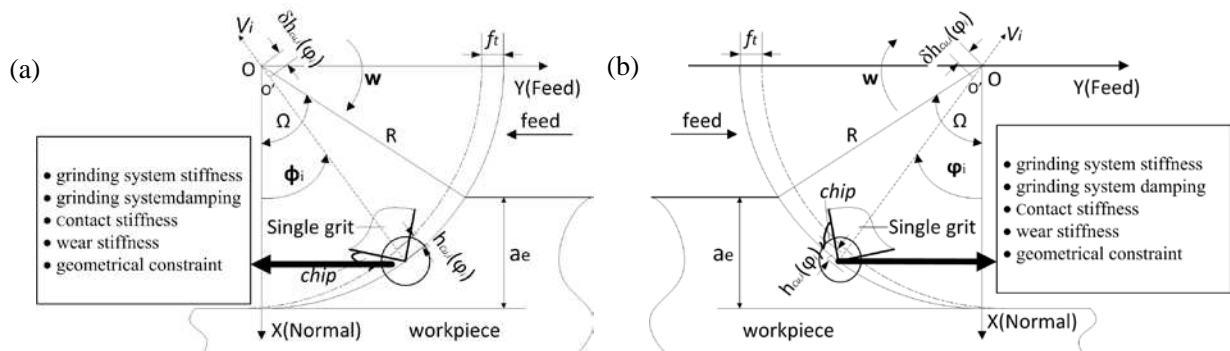

Fig.2   **a** Down grinding and **b** Up grinding considering eccentricity of wheel ($\delta h_{cu,i}(\varphi_i)$)

（1） When down grinding，similar geometry of a quarter of abrasive wheel is modeled as shown in Figure2(a)，the instantaneous chip thickness of single grit in grinding-in is calculated as:

$$h_{cu,i}(\varphi_i) = \begin{cases} h_{cu,0} + \Delta h_{cu,i} + \delta h_{cu,i}(\varphi_i) & 0 \leq \varphi_i \leq \Omega \\ 0 & other \quad area \end{cases} \quad (1)$$

（2） When up grinding, similar geometry of a quarter of abrasive wheel is modeled as shown in Figure2(b)，the instantaneous chip thickness of single grit in grinding-in is calculated as:

$$h_{cu,i}(\varphi_i) = \begin{cases} -h_{cu,0} + \Delta h_{cu,i} + \delta h_{cu,i}(\varphi_i) & -\Omega \leq \varphi_i \leq 0 \\ 0 & other \quad area \end{cases} \quad (2)$$

Where $h_{cu,0}$ is static chip thickness and is calculated as $h_{cu,0} = f_t \sin(\varphi_i)$, f_t is the feed per revolution of studied grit. It is an important intermediate variable of grinding dynamics. $\Delta h_{cu,i}$ is dynamic chip thickness in radial direction derived from regenerative vibration and will be calculated in next section 2.2. $\delta h_{cu,i}(\varphi_i)$ is named as dynamic chip thickness deviation excited by eccentrically rotational behaviour of grinding wheel or machine tool spindle. Its exciting principle and model are further deduced in section 2.3. Variable φ_i is rotational position angle of single grit in Z-axial plane and is depicted as: $\varphi_i = \Omega - \theta$, $\theta = \omega T$ is calculated as rotational angle of spindle of abrasive wheel with angular velocity ω within a consecutive grit time interval T. Ω is entire included angle of grit cutting-in and cutting-out interaction zone and is calculated as:

$$\Omega = \arccos \frac{R - a_p}{R} \quad .$$

2.2 Regenerative vibration mechanism of chip formation

Considering the motion in radial direction, grinding regenerative vibration is depicted in Figure 3 as continuously relative movement between abrasive grit and workpiece in chip cross-sectional area. The vibration is excited by difference of the phase magnitude (theoretical magnitude $H_{cu,0}(t)$ by not considering any self-exciting factors and actual magnitude $H_{cu}(t)$ excited by regenerative behaviour) and angle deviation(Ψ) in Figure 3 between two subsequent finished surface undulations($y(t-T)$ and $y(t)$), which results in additional chip thickness, namely effect of grinding chip thickness variation.
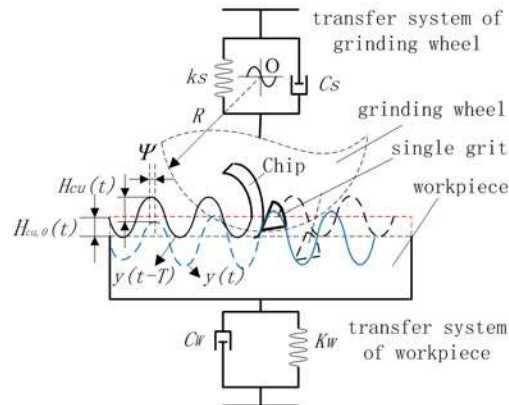

Fig.3　Regenerative chip formation of workpiece-wheel interaction in feed direction

Effect of regenerative mechanism is great on instantaneous chip formation and further on micro-grinding force of each grit. During down-grinding process, $\Delta h_{cu,i}$ is dynamic displacement of workpiece-abrasive grit contact system in radial direction derived from regenerative vibration tracks in interactive grinding zone of single grit i. It is characterized as:

$$\Delta h_{cu,i} = (H_{is}(t-T) - H_{is}(t)) - (H_{iw}(t-T) - H_{iw}(t)) \tag{3}$$

Where $H_{is}(t)$, $H_{is}(t-T)$, $H_{iw}(t)$, $H_{iw}(t-T)$ are respectively dynamic displacements of the current and previous grit-workpiece pairs in radial direction at instantaneous same position angle φ_i under regenerative vibration conditions. All four variables are deduced in the subsequent analysis and are transferred from vectors with Cartesian coordinate in Figure 2 as:

$$H_i(t) - H_i(t-T) = (X_i(t) - X_i(t-T)) \cos\varphi_i + (Y_i(t) - Y_i(t-T)) \sin\varphi_i \tag{4}$$

2.3 Eccentrically rotational model of grinding wheel

The typical eccentrical model of abrasive wheel is illustrated in Figure 4. Reference coordinate centre O′ is machine tool spindle rotational centre. Reference coordinate centre O is actual rotational centre of grinding wheel. Variable $\delta_e = \overline{OO'}$, characterized as wheel eccentricity value, can be pre-measured and examined in dynamic balancing experiment (using a tactile measuring sensor on the inspection).
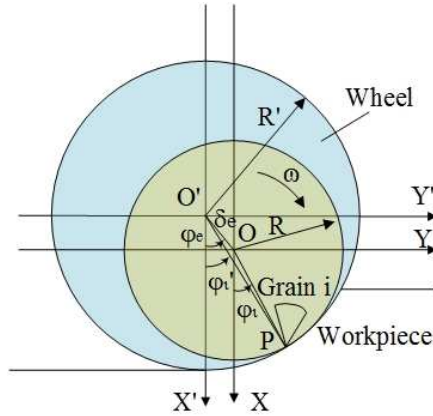

Fig. 4 Eccentrically rotational model of grinding wheel ($\delta_e = \overline{OO'}$,o'-spindle axis, o-actual wheel axis)

Variable $\delta h_{cu,i}(\varphi_i)$ is dynamic chip thickness deviation excited by wheel eccentrically rotational behaviour and approximately evaluated as:

$$\delta h_{cu,i}(\varphi_i) = R_i'(\varphi_i') - R_{i-1}'(\varphi_i') \tag{5}$$

Where $R_i'(\varphi_i')$ and $R_{i-1}'(\varphi_i')$ are respectively presented as the grinding radius of the current and previous working grits in contact zone. As shown in Figure 4, $R_i'(\varphi_i')$ is calculated as:

$$R_i'(\varphi_i') = \sqrt{R^2 + \delta_e^2 - 2R\delta_e \cos(\angle O'OP)} \tag{6}$$

$$\angle O'OP = \pi - |\varphi_i - \varphi_e|$$

Where φ_e is relative position angle with actual wheel rotational centre, which is described as: $\varphi_e = \varphi_{ei0} - \theta$, φ_{ei0} is initial position angle of studied grit i distributed on abrasive wheel that depends on clamped position and is measured in preparation phase prior to grinding process. By putting these parameters into equation (6), $R_i{}'(\varphi_i')$ becomes:

$$R_i{}'(\varphi_i') = \sqrt{R^2 + \delta_e^2 - 2R\delta_e \cos(\pi - |\Omega - \varphi_{ei0}|)} \tag{7}$$

2.4 Close-loop feedback control system with regenerative mechanism

As proposed dynamics models illustrated in Figure 2 and Figure 3, the ideal structural models for surface grinding process in the paper is assumed as a spring-mass-damper vibratory system with two-degree-of-freedom in the two mutually perpendicular X(normal) and Y(feed) directions. Dynamics equation of surface grinding process at a discretional time t is characterized as [6,14]:

$$\begin{cases} F_x(t) = m_x\ddot{x}(t) + c_x\dot{x}(t) + k_x x(t) \\ F_y(t) = m_y\ddot{y}(t) + c_y\dot{y}(t) + k_y y(t) \end{cases} \tag{8}$$

where F_x, F_y are the total grinding forces accumulated by force acting on each abrasive grit. m, c, k are modal mass, damping and stiffness values of abrasive machining tool at the chip cross-sectional area in the feed or normal directions and can be obtained with modal experimental data. $x(t)$, $y(t)$ represent relatively displacements in abrasive grit-workpiece interaction vibration system in normal and feed directions respectively.

During regenerative grinding in Figure 3, instantaneous cutting force acting on current single grit excites vibration increment of abrasive wheel and workpiece separately based on regenerative vibration mechanism in the normal (X) and feed (Y) directions periodically, which then causes to dynamic displacements (directly relative with undeformed chip thickness) changes Δx and Δy respectively that are all major variables in analytical increment model of grinding force. So the force and regenerative vibration interact mutually and construct a closed-loop feedback system, as illustrated in Figure 5.

In Figure 5, after doing Laplace transform, $H_{cu,0}(s)$ is same as the kinematic undeformed chip thickness $h_{cu,0}$ that is depicted in Equation (1) and (2), and $H_{cu}(s)$ is the final grinding chip thickness which is the sum of above-mentioned kinematic and dynamic vibratory displacements derived from regenerative vibration and wheel eccentric behaviour in abrasive wheel-workpiece interaction system. μ and T are respectively overlap coefficient and time interval between the current and adjacent ground surface undulation gained by working grits. [$G_{xx}^c(s)$、 $G_{xy}^c(s)$、 $G_{yx}^c(s)$、 $G_{yy}^c(s)$]and[$G_{xx}^w(s)$、 $G_{xy}^w(s)$、 $G_{yx}^w(s)$、 $G_{yy}^w(s)$] that can be identified and restructured with experimental data collected by standard modal tests are applied with respectively direct and cross transfer function models of wheel-workpiece vibration system in the normal(X) and feed(Y) directions.
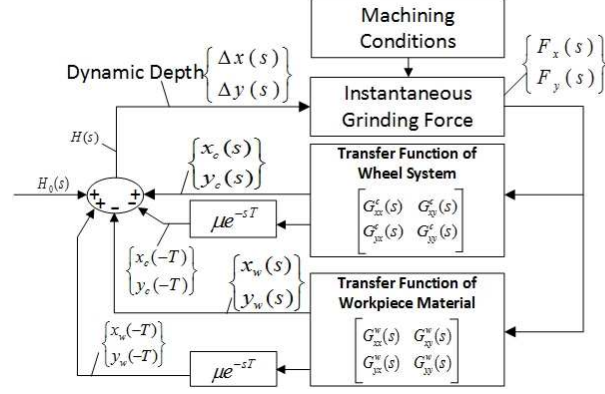
Fig. 5 Close-loop control system of regenerative workpiece-wheel interaction process

As depicted in Figure 5，dynamic incremental displacements of abrasive grits and workpiece in Laplace transfer domain are calculated as:

$$\begin{Bmatrix} \Delta x_c \\ \Delta y_c \end{Bmatrix} = (1 - \mu e^{-sT}) \begin{bmatrix} G_{xx}^c(s) & G_{xy}^c(s) \\ G_{yx}^c(s) & G_{yy}^c(s) \end{bmatrix} \begin{Bmatrix} F_x \\ F_y \end{Bmatrix} \tag{9}$$

$$\begin{Bmatrix} \Delta x_w \\ \Delta y_w \end{Bmatrix} = (1 - \mu e^{-sT}) \begin{bmatrix} G_{xx}^w(s) & G_{xy}^w(s) \\ G_{yx}^w(s) & G_{yy}^w(s) \end{bmatrix} \begin{Bmatrix} F_x \\ F_y \end{Bmatrix} \tag{10}$$

In Equation (9) and (10), due to considering regenerative mechanism, regular process parameters that are all included in the analytical force model, such as circumferential speed of wheel spindle, workpiece speed in feed direction and increasing underformed chip thickness that are mostly considered as linear constants in simplified models are transferred and evolved to nonlinear variables, which make dynamics results of wheel-workpiece vibration system more accurate and practical for the process control purpose.

2.5 Differential model of grinding force acting on single grit unit

Mathematical model of grinding force and relevant geometrical correlation of abrasive grit-material are shown in Figure 6 [20]. In material removal process, axial grinding force is negligible due to grit non-bias random orientation, which results to only little effect on grinding stability and ground surface of workpiece. The ploughing and friction forces are not taken into account to avoid non-necessary complexity of secondary influences. The material removal is approximated as a pure shear process with a conical grinding grain.
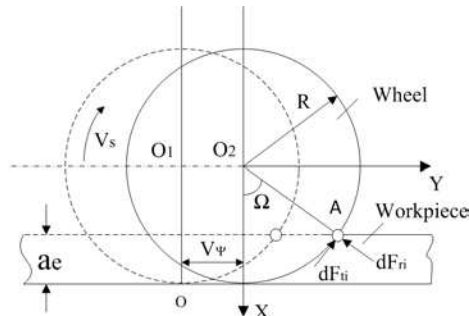

Fig. 6 Machining schematic of single working abrasive grit [20]

One individual abrasive grit 'A' located in initial grinding-in position is selected and assumed with same typical shape of pyramid as shown in Figure 2. Instantaneous grinding force acting on grit 'A' in shear plane that is normal to wheel rotational axis are the resultant of tangential force dF_{ti} and radial force dF_{ri}, and is evaluated by using Werner's grinding force model [20]:

$$\begin{bmatrix} \mathrm{d}F_{ti}(\varphi_i) \\ \mathrm{d}F_{ri}(\varphi_i) \end{bmatrix} = \begin{bmatrix} K_s \\ c_s K_s \end{bmatrix} \left[v_w / v_s \right]^{2\varepsilon-1} \left[d_s \right]^{1-\varepsilon} h_{cu,i}(\varphi_i) \, \mathrm{d}\varphi \qquad (11)$$

where K_s is defined as specific grinding force in per unit chip area considering distribution density, protrusion height and negative rake angle of abrasive grits mounted on wheel surface at micro-grinding condition, calculated as: $K_s = P_m/(ba_ev_s)$, P_m is specific grinding energy of removing material per unit volume, c_s is grinding force ratio in tangential and radial directions. Both of above variables that are also determined by wheel sharpness, workpiece material property and grinding behaviours can be obtained from experimental data. v_w is feed speed of workpiece, v_s is peripheral speed of grinding wheel. d_s is wheel diameter. $h_{cu,i}(\varphi_i)$ is the instantaneous grinding chip thickness as depicted in Equation 1 during down-grinding. φ_i is rotational position angle of individual abrasive grit as shown in Figure 2. The constant ε is comprehensive influential coefficient of individual grit 'A' friction behaviour and approximately set with 1 in a pure shear process.

Instantaneous grinding forces calculated in Equation (11) respectively are projected to the Cartesian coordinate system in the normal (X) and feed (Y) directions as:

$$\begin{bmatrix} \mathrm{d}F_{xi} \\ \mathrm{d}F_{yi} \end{bmatrix} = \begin{bmatrix} -\sin\varphi_i & -\cos\varphi_i \\ \cos\varphi_i & -\sin\varphi_i \end{bmatrix} \begin{bmatrix} \mathrm{d}F_{ti}(\varphi_i) \\ \mathrm{d}F_{ri}(\varphi_i) \end{bmatrix} \qquad (12)$$

By combining and integrating Equations (1)-(3), (10) and (12), instantaneous grinding force acting on single grit 'A' in down grinding process are obtained. Then total grinding force in given per rotational period will be summed up as shown in Equation 13 by accumulating the force from each active individual kinematic grit that is effective in abrasive grit-material interaction zone to remove material. Here n is active grit numbers with specific instantaneous undeformed chip thickness in the interaction zone.

$$\begin{cases} F_x(t) = \sum_{i=1}^{n} dF_{xi} \\ F_y(t) = \sum_{i=1}^{n} dF_{yi} \end{cases} \qquad (13)$$

3. Quantitative assessment of grinding system stability

3.1 Machining conditions and test method

For the analysis of the comprehensive effects on grinding dynamics, a series of grinding conditions are designated in Table 1 and an experimental platform with integrated measurement devices is shown in Figure 7. In order to analyse the influence of the negative rake angle and dynamic eccentricity of wheel, the experiments were carried out with other machining parameters remained unchanged. All measurement of grinding dynamics tests was conducted on a surface grinding machine tool MSG-250HMD whose table length and width range is 480*200mm. The traversing speed of the machine in feed direction is 5-20m/min. Grinding spindle speed range is

500-4000*r.p.m.* A piezoelectricity grinding dynamometer Kistler 9257BA that connects with a dynamic signal analyser Dewe2010 and a computer is installed to collect grinding force signals, as shown in Figure 7. The sampling frequency is set to be 50*KHz.*

Table 1 Designated machining conditions

| Constant parameters	unit	value
Grinding kinematics		Down grinding
Wheel type		Electroplated diamond
Workpiece material		EN8
Abrasive grit average size	um	300
Dominant grit geometry		Pyramid
Grit distribution feature		Normal distribution in feed direction
Grit distribution density	$/mm^2$	0.64
Wheel diameter	mm	150
Wheel width (b)	mm	20
Grinding wheel cutting speed (v_s)	m/s	35
Grinding depth	um	20
Total grinding depth	mm	1
Grinding width	mm	5
Specific grinding energy	$J.mm^{-3}$	20
Grinding force ratio (Ft/Fn)		0.35
Feed rate of workpiece	mm/s	200
Cooling and lubricating		dry
Incremental parameters	**Unit**	**value**
Dynamic eccentricity of wheel	um	1,2,3,4,5
Negative rake angle of grit	$degree$	-15,-30,-45,-60,-75
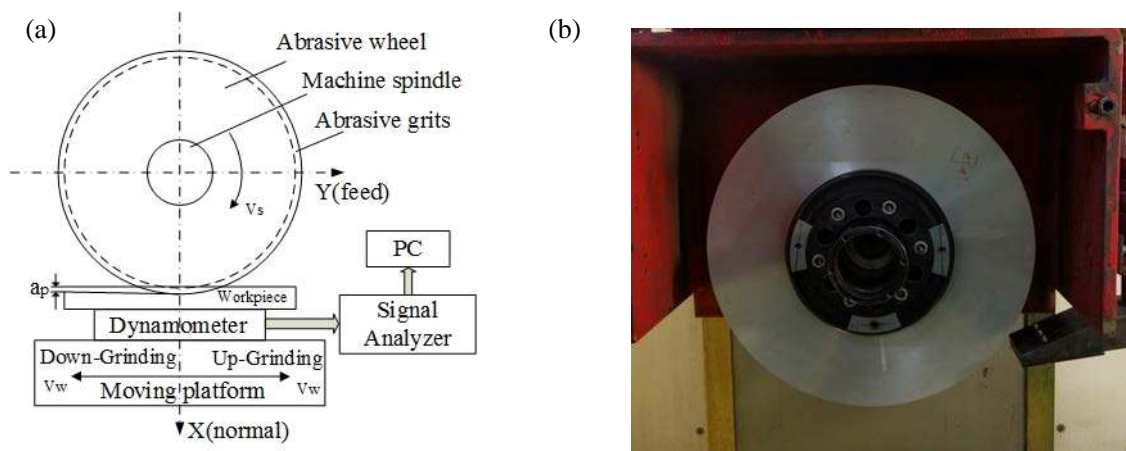
Fig. 7 a Test platform of abrasive grinding dynamics**, b** Surface grinding wheel

3.2 Comparison analysis of test and simulation dynamics results

To validate the effectiveness and accuracy of mathematical models of derivative grinding force as Equation (11) and Equation (12), five groups of tests are conducted with given machining conditions as shown in Table 1. The mean values of peaks and bottoms of specific force signals in each periodical revolution are extracted in absolute value range with 2 *ms* interval in the five groups of tests. The simulated and experimental results of specific grinding forces with grinding width of 1 *mm* in normal and feed directions are illustrated in Figure 8. It shows a good agreement of specific grinding force in both directions between the experiments and simulation. All deviation ratio of dynamics curves caused by influence factors of self-excited and forced-excited vibration system are presented in subsequent section 3.4.
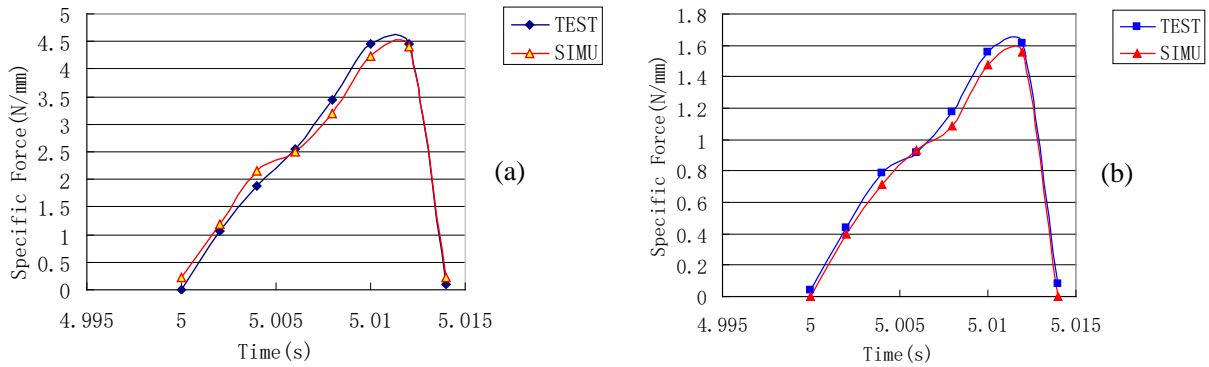

Fig. 8 Experimental and the simulated specific force during down-grinding

a in normal direction and **b** in feed direction(a_e=20um, v_s=35m/s, v_w=200mm/s, dry)

3.3 Kinetic undeformed chip thickness distribution of working grits

The undeformed chip thickness distribution of active working grits in the grit-material interaction (contact) zone is very important for grinding dynamics research in terms of grinding process behaviour and wheel topography variation and wheel life [21]. Due to irregular characters of grits distribution, such as grit size, geometry shape, protrusion height and distribution density, actual measurement of undeformed chip thickness distribution is difficult and not satisfactory in practice yet.

The undeformed chip thickness depends on the workpiece material, the machining conditions, the friction conditions between abrasive grit and workpiece and the shape of the grits. For the analysis of kinetic undeformed chip thickness distribution, matrix information of each grit that includes average size, distribution pattern, protrusion height, spacing distance or distribution density, are collected or assumed as listed in Table 1. Complied with Equations (1) and (2), the calculated results of kinetic undeformed chip thickness distribution-frequency (i.e. active grit numbers with specific undeformed chip thickness) in grit-workpiece interaction zone along normal direction under given machining conditions in Table 1 is illustrated as Figure 9.
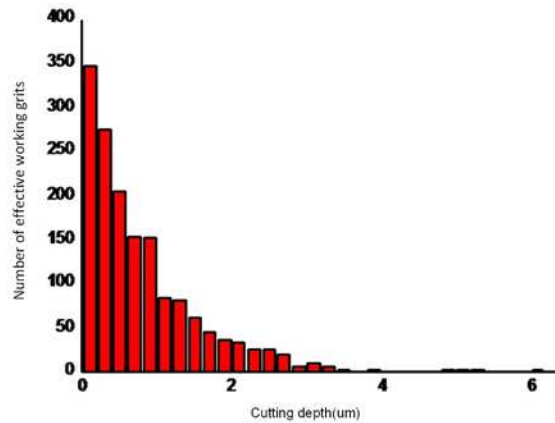
Fig. 9 Cutting depth distribution of active grits at depth of cut of 20 *um*

3.4 Analysis considering dynamic eccentricity of abrasive wheel

In actual grinding process, assembly or remounting oscillation excited from machine tool spindle and grinding wheel cannot be neglected even with high-stiffness grinding machine and high quality conditioned wheel. This results in the variation of undeformed chip thickness in contrast to the ideal process during the material removal process. Eccentric deviation of wheels can be minimized even eliminated prior to grinding with dressing or reconditioning technique, as well as dynamic balancer with the aid of some specific devices. The eccentricity values of electroplated diamond wheels are examined by utilizing dynamic balancer NHY-2000-810A , as shown in Figure 10. Rotating speed range of the balancer is 120-10000 *r.p.m*. Minimum residual eccentricity is about 0.1-0.5*um* after dynamic balancing.
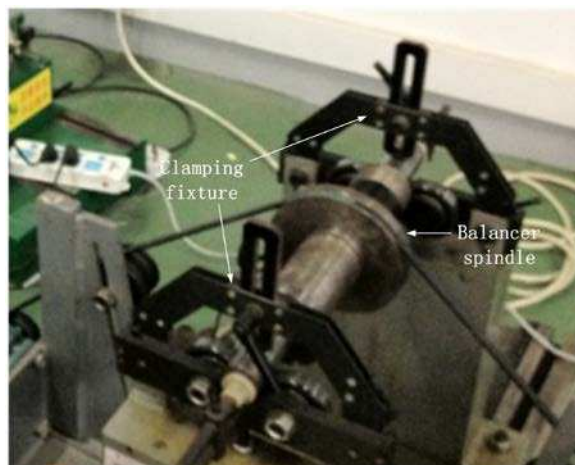

Fig. 10 Measurement device of dynamic balancer

As one of the influential factors of undeformed chip thickness, the eccentricity values are used to analyse their effects on the instantaneous undeformed chip thickness and then on grinding forces, as well as on vibration of abrasive grit-material interactions. The change ratios of grinding force and vibration of abrasive grit-workpiece under incremental machining conditions are calculated respectively as:

$$\xi_{Fx} = \frac{F_{xi} - F_{x0}}{F_{x0}}, \quad \xi_{Fy} = \frac{F_{yi} - F_{y0}}{F_{y0}} \tag{14}$$

$$\xi_{\Delta x} = \frac{\Delta x_i - \Delta x_0}{\Delta x_0}, \quad \xi_{\Delta y} = \frac{\Delta y_i - \Delta y_0}{\Delta y_0} \tag{15}$$

Where, F_{x0}, F_{y0}, Δx_0 and Δy_0 are respectively reference values of grinding forces and vibrations in normal and feed directions with wheel eccentricity value of zero.

The changing curves are illustrated with maximum and minimum magnitudes of simulated grinding force that typically illustrate the grinding moments in each revolution period with maximum and minimum undeformed chip thickness $h_{cu,i}$, as well as simulated vibration of abrasive grit-material interactions in relation to the dynamic eccentricity of wheel are shown in Figure 11 and Figure 12 under machining conditions as shown in Table 1. In both figures, change ratios on force and vibration show the upwards trend with the increase of the wheel eccentricity.

Comparing to the ideal process in which wheel eccentricity value is set with zero, the mean changing ratio of grinding forces in feed and normal directions derived from abrasive wheel eccentricity of 1um that is regular limitation value when abrasive wheel is fixed with machine spindle under stable precision grinding in industry increases to 7.5%, 3.3%, as well as to 2.3%, 0.28% on vibration in feed and normal directions. Because the change ratios of entire machining dynamics are under 10%, force-excited mechanism resulted from wheel eccentric behaviour is seldom considered in dynamics analysis.
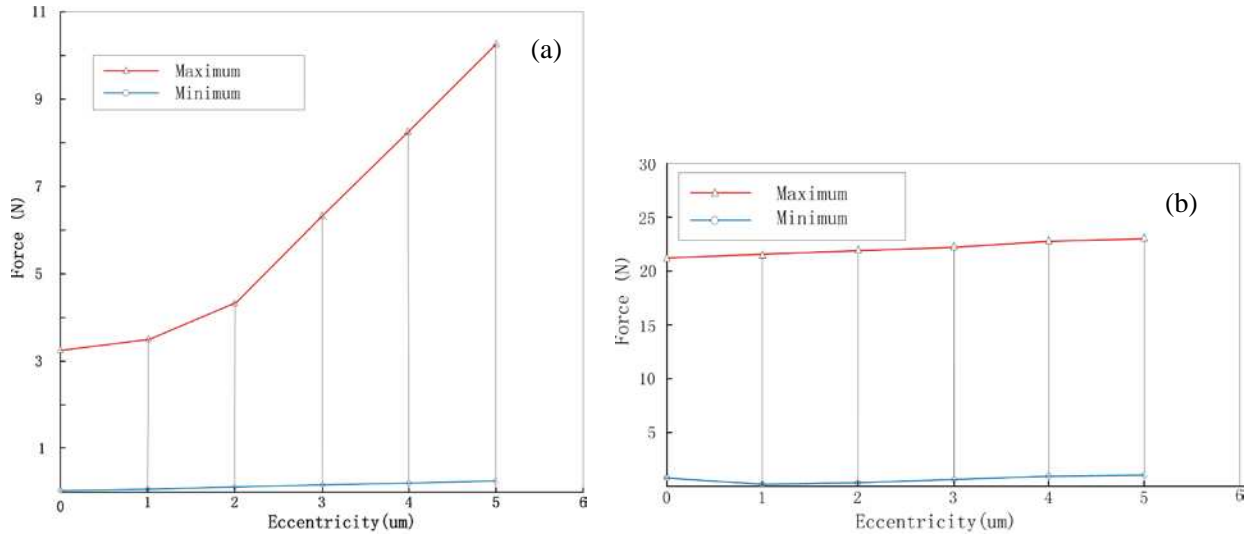

Fig. 11 Grinding force **a** in feed direction and **b** in normal considering dynamic eccentricity of abrasive wheel
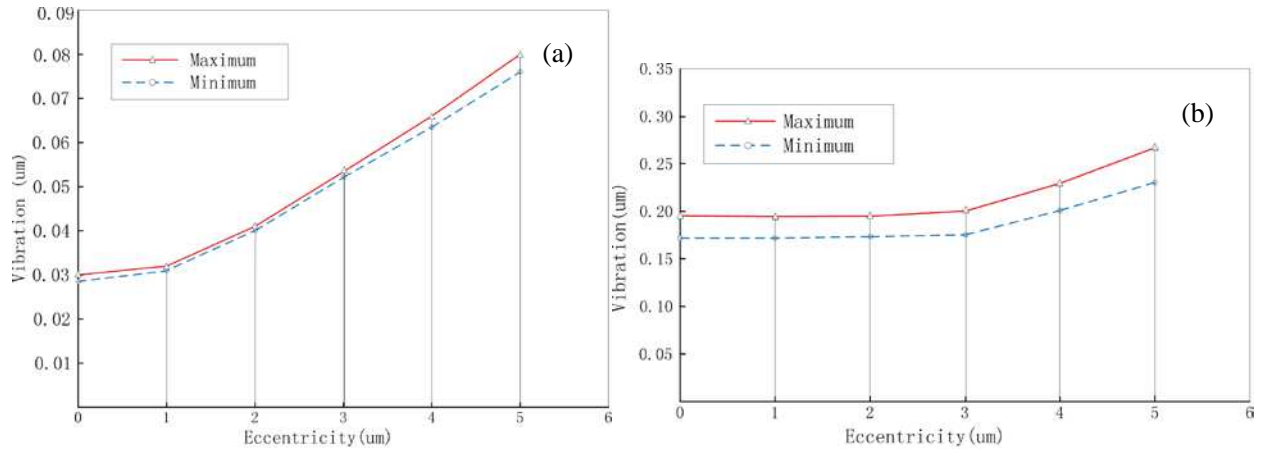
Fig. 12 Grinding vibration **a** in feed direction and **b** in normal direction considering dynamic eccentricity of abrasive wheel

Quantitative assessment threshold of effect of change ratio at incremental wheel eccentricity on machining stability are presented in Table 2. At the threshold of wheel eccentricity value that is over 2*um*, even up to maximum 3*um* that is regular limitation value during coarse grinding, a slight change of wheel eccentricity (1*um*) has resulted to a greater change ratio (a change ratio of over 90% in a sharp growing is observed at eccentricity value of 3*um*)on grinding force, as well as vibration in feed direction. Under the condition, machining process has to be interrupted as severe forced vibration, even chatter of abrasive grit-material system occurs. Accordingly, the change ratio of force in feed direction under the wheel eccentricity of 5*um* is nearly 2 times larger than the kinematic force in the low range of value of under 1 *um*.

Table 2 Change ratios of force and vibration at incremental wheel eccentricity

ξ(%) δe (*um*)	grinding force		vibration	
	Feed direction	Normal direction	Feed direction	Normal direction
1	7.5	3.3	2.3	0.28
2	32	6.9	33.6	0.9
3	94	11.5	75	6.7
4	154	14.8	116.6	24.3
5	215	18.8	158	42

Especially, the influence magnitude on grinding force in feed direction is obviously much greater than that in normal direction due to diverse kinematics constraints. Similar situation is depicted on grinding vibration. This is explained by the fact that grinded workpiece material around grits is suppressed down to working platform in normal direction during down-grinding, change derived from wheel eccentric mechanism facilitates larger vibration in feed direction and thus increases instability in feed direction.

Thereby, analysis results show that the wheel eccentricity should be controlled in the range of 1*um* to 2*um*, and limited under maximum value of 3*um* to ensure machining stability. The greater eccentricity of wheel results in the larger average change of force and vibration (an increase of 94% of force and 75%of vibration in feed direction) for an unstable grinding process.

3.5 Analysis considering negative rake angle of working grits

Many experiments applied with a series of varying regular machining conditions [14, 16] have shown that grits or cutters edges with an increasing negative rake angle whose value is up to limitation -75 *degree* (apex angle is 150 *degree* in scratching direction) leads to higher plastic material deformation and is still in work condition with cutting mode and can make the chip in contact zone formed. But those worn edges of abrasive grits with negative rake angle whose limitation values are measured to be -85 *degree* (top wedge angle is 170 *degree*) are only work in scratching and ploughing phases, which results in only severe plastic deformation and pile-up phenomena of flowing localized material rather than chip formation from rake face of cutting edges, as well as during the entire engagement.

Variations in grit geometry would significantly influence the cross-section situation during the cutting process. In order to evaluate the ability to determine the influence of varying negative rake angles, five incremental levels were applied as listed in Table 1.

The resulting maximum and minimum curves of grinding force deviation, as well as vibration deviation of grit-material system regarding negative rake angle of grit are shown in Figure 13 and Figure 14. Quantitative assessment threshold of effect of change ration of force and vibration at incremental negative rake angle of abrasive grit on machining stability are presented in Table 3 by comparing with the reference values of force and vibration with grit negative angle value of zero. A reduced level of negative rake angle (i.e. increased absolute values) with the same grit diameter leads to an increased applicable maximum undeformed chip thickness, and further facilitates slightly increasing of grinding force and vibration. Most of change ratios are less than 50% (the threshold of change ratio occurs at a sharp edge with rake angle, e.g. -30 *degree* to -45 *degree*). Moreover, it was found that when at the larger values of negative rake angle of working grit (e.g. over -75 *degree*), relatively the rake face of grit is strongly inclined to the material surface. Thus, a greater proportion of the material is displaced below the workpiece surface and severe plastic upheaval on both sides. Grinding force and vibration of grit-material system keep almost unchanged. The result agrees with the conclusion of the research [21, 22, 23, 24].

Table 3 Change ratios of force and vibration at incremental negative rake angle of abrasive grit

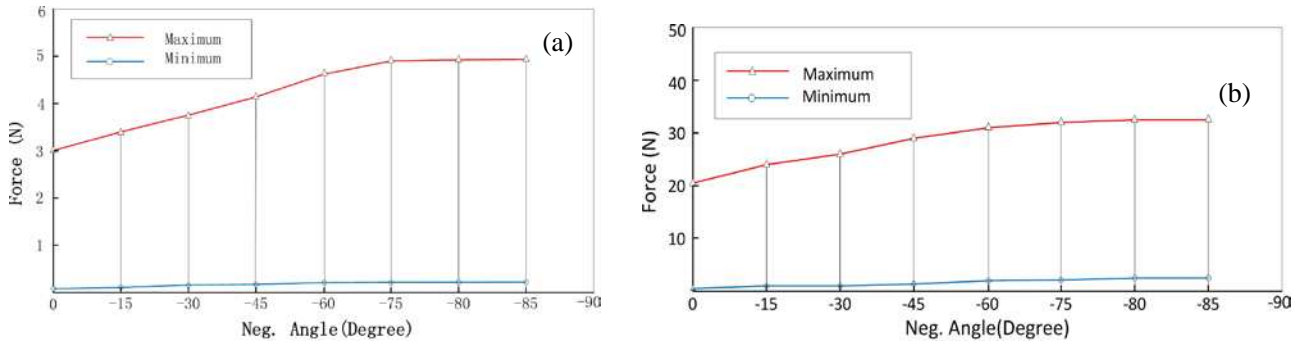| $\xi(\%)$ / $\gamma_0(degree)$	grinding force		vibration	
	Feed direction	Normal direction	Feed direction	Normal direction
-15	7.4	7.36	7.5	7.35
-30	18	18	18	17.8
-45	28.3	28.3	28	28
-60	37.4	37.3	36.8	36.8
-75	44	44	43.3	43.3
-80	45	45.3	44.6	44.6
-85	46	46	45.4	45.4

Fig. 13 Grinding force **a** in feed direction and **b** in normal direction considering varying negative rake angle of grits edges
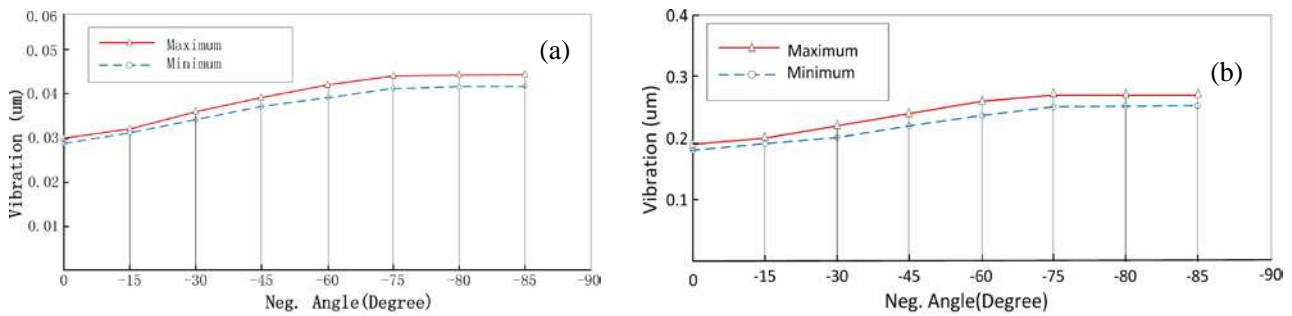

Fig. 14 Grinding vibration **a** in feed direction and **b** in normal direction considering varying negative rake angle of grits edges

4. Conclusion

Instantaneous undeformed chip thickness is a very important and nonlinear intermediate variable for the development of a new set of nonlinear dynamics models of grinding in consideration of the regenerative vibration mechanism and the dynamic eccentric influence on grinding performance. The analytical models presented in the paper provide more accurate insight of dynamics characteristics than some existing simplified models. More nonlinear influence factors, such as friction, grit wear, material properties etc, can be taken into account of the variation of undeformed chip thickness in the models. Based on the results introduced within the paper, the following conclusions can be drawn.

1. The qualitative and quantitative assessment of machining stability demonstrated that the change ratios of grinding force and vibration increase significantly when the wheel eccentricity is higher than 2 um. This gives a good guidance to the grinding machine design.

2. The change ratios of grinding force and vibration increase significantly when negative rake angle of abrasive cutting edge changes from 0° to -60°. Further increase negative rake angle may not make a significant increase of the change ratios of grinding force and vibration.

References

1. Aurich JC, Kirsh B (2012) Kinematic simulation of high-performance grinding for analysis of chip parameters of single grits. CIRP Journal of Manuf Sci Technol 5:164-174
2. Li XK, Wolf S, Zhu TX, Zhi G, Rong YM (2015) Modeling and analysis of the bonding mechanism of CBN grit

for electroplated superabrasive tools—Part 1: introduction and application of a novel approach for determining the bonding force and the failure modes. Int J Adv Manuf Technol 76:2051-2058

3. Li XK, Wolf S, Zhu TX, Zhi G, Rong YM (2015) Modeling and analysis of the bonding mechanism of CBN grit for electroplated superabrasive tools—Part 2: finite element modeling and experimental verification. Int J Adv Manuf Technol 77:43-49

4. Darafon A, Warkentin A, Bauer R (2013) 3D metal removal simulation to determine uncut chip thickness, contact length and surface finish in grinding, Int J Adv Manuf Technol 66:1715-1724

5. Chen X, Öpöz TT(2014) Characteristics of material removal processes in single and multiple cutting edge grit scratches, Int J Abr Technol 6 : 226-242

6. Malkin S, Cai GQ (2002) Grinding technology theory and applications of machining with abrasive (in Chinese). Northwestern University Press, Xi'an, China

7. Inasaki I, Karpuschewski B, Lee H(2001) Grinding chatter-origin and suppression. Annals of CIRP Manuf Technol 50:515-534

8. Altintas Y, Weck M(2004) Chatter stability of metal cutting and grinding. Annals of CIRP Manuf Technol 53:619-642

9. Jiang JL, Ge PQ, Hong J(2013) Study on micro-interacting mechanism modelling in grinding process and ground surface roughness prediction. Int J Adv Manuf Technol 67:1035-1052

10. Fu YC, Tian L, Xu JH, Yang L, Zhao JY (2015) Development and application on the grinding process modeling and simulation. J Mech Eng 51: 198-205

11. Hou ZB, Komanduri R(2003) On the mechanics of the grinding process-part I, Stochastic nature of the grinding process. Int J Mach Tools Manuf 43:1579-1593

12. Agarwal R, Rao PV(2012) Predictive modeling of undeformed chip thickness in ceramic grinding. Int J Mach Tools Manuf 56:59-68

13. Linke BS (2015) A review on properties of abrasive grits and grit selection. Int J Abra Technol 7:46-58

14. Ren JX, Kang RK, Shi XK (1992) Grinding technology of difficult-to-machine materials (in Chinese). National Defence Industry Press, Beijing, China

15. Ren JX, Hua D (2011) Grinding principle(in Chinese). Publishing House of Electronics Industry, Beijing, China

16. Badger J, Murphy S, O'Donnell G(2011) The effect of wheel eccentricity and run-out on grinding force, waviness, wheel wear and chatter, Int J Mach Tools Manuf 51:766-774

17. Aurich JC, Herzenstiel P, Sudermann H, Magg T (2008) High-performance dry grinding using a grinding wheel with a defined grit pattern. Manuf Technol 57:357-362

18. Axinte D, Butler-Smith P, Akgun C, Kolluru K (2013) On the influence of single grit micro-geometry on grinding behavior of ductile and brittle materials. Int J of Mach Tools Manuf 74:12-18

19. Rasim M, Mattdeld P, Klocke F (2015) Analysis of the grit shape influence on the chip formation in grinding, J Mater Process Technol 226:60-68

20. Werner G (1978) Influence of work material on grinding force. Annals of CIRP 27: 243-248

21. Yu TB, Zhang JQ, Peng G, Wang WS (2010) Investigation of grinding process simulation, Adv Mater Res 126-128:119-124

22. Huang H, Lin SH, Xu XP (2010) Study on Grinding forces for glass grinding with single diamond grit(in Chinese). China Mechan Eng 21: 1278-1282

23. Klocke F, Barth S, Mattfeld P (2016) High performance grinding. 7th HPC 2016-CIRP Conf High Performance cutting 46: 266-271

24. Winter M, Ibbotson S, Kata S, Hermann C (2015) Life cycle assessment of cubic boron nitride grinding wheels. J Cleaner Production 107: 707-721